OPEN ACCESS
OPUS AUGSBURG

Universität Augsburg
Universitätsbibliothek

Understanding the gas phase formation of silicon carbide during reactive melt infiltration of carbon substrates

Manikanda Priya Prakasan, Tobias Schneider, Dietmar Koch

Angaben zur Veröffentlichung / Publication details:

Prakasan, Manikanda Priya, Tobias Schneider, and Dietmar Koch. 2025. "Understanding the gas phase formation of silicon carbide during reactive melt infiltration of carbon substrates." Open Ceramics 22: 100767. https://doi.org/10.1016/j.oceram.2025.100767.

Nutzungsbedingungen / Terms of use: **CC BY-NC 4.0**

Dieses Dokument wird unter folgenden Bedingungen zur Verfügung gestellt: / This document is made available under these conditions:
CC-BY-NC 4.0: Creative Commons: Namensnennung - Nicht kommerziell
Weitere Informationen finden Sie unter: / For more information see:
https://creativecommons.org/licenses/by-nc/4.0/deed.de

Open Ceramics 22 (2025) 100767

Contents lists available at ScienceDirect

Open Ceramics

journal homepage: www.sciencedirect.com/journal/open-ceramics

Understanding the gas phase formation of silicon carbide during reactive melt infiltration of carbon substrates

Manikanda Priya Prakasan *, Tobias Schneider, Dietmar Koch

Institute of Materials Resource Management, University of Augsburg, Am Technologiezentrum 8 86159 Augsburg, Germany

ARTICLE INFO

Keywords:
C/C-SiC composite
Reactive Melt Infiltration
Liquid Silicon Infiltration
Surface siliconization
Gas phase SiC formation

ABSTRACT

Carbon-Carbon composites with protective Silicon Carbide surface (C/C-SiC) are well-known for their exceptional heat and oxidation resistance. Reactive Melt Infiltration (RMI) is employed to impart oxidation resistance to these composites by transforming the carbon matrix surface into silicon carbide. Successful infiltration yields dense-grey SiC, while unsuccessful process yields porous-green layer, compromising oxidation resistance and inducing high-temperature surface damage. Identifying the causes of failed siliconization and their influencing factors is crucial for enhancing high-temperature performance. This study proves that SiC formation from gas-phase reactions prior to silicon melting causes green surface layer. Through siliconization experiments and Thermogravimetric Analysis combined with Fourier Transform Infrared spectroscopy, these gaseous reactions are linked to the specific-surface characteristics of silicon powder used. Microstructural differences between gas and liquid reaction-formed SiC leads to the proposed four-step reaction pathway, explaining the formation of green SiC. These findings offer vital insights for optimizing the outcome of surface siliconization process.

1. Introduction

Carbon Fiber Reinforced Carbon Matrix composites (C/C) have found extensive use in the space industry, where the application requires excellent high temperature resistant materials in combination with light weight characteristics. Although the C/C composites exhibit superior toughness in comparison to the monolithic graphite, their oxidation resistance is no more superior. For applications requiring extended periods of operation in an oxidizing environment at temperatures above 450 °C (for e.g. nose cone and wing edges of space shuttles), an additional protection is required [1–3]. The most extensively used method involves forming a silicon carbide outer surface on the C/C composite to prevent oxygen from attacking the carbon substrate [4]. These Carbon Fiber Reinforced Carbon Matrix composites with Silicon Carbide (SiC) surface (C/C-SiC) have gained enormous attention in the space industry. Reactive Melt Infiltration using silicon, also known as Liquid Silicon Infiltration (LSI) is one of the methods that is successfully demonstrated to produce a protective SiC surface on the composites, which reduces the oxidation rate and enhances the high temperature resistance. Ideal outcome of the surface siliconization process is a dense SiC surface (grey in color) with strong adhesion to the substrate. However, sometimes, the siliconization could result in a "green" surface layer that has very weak bonding to the composite surface. This green layer is proven by Hofbauer and Raether to be a purer form of SiC using X-ray fluorescence analysis (XRF). These components with failed green SiC surface ultimately have poor oxidative resistance during service [5]. In a typical industrial process, the siliconized components are visually assessed and the presence of porous or peeling green surface layer is assigned as a "Failed Siliconization" process. These components need to be re-processed until a satisfactory SiC surface is obtained. This re-processing leads to increased production costs and longer manufacturing times. Hence it is necessary to understand the mechanism behind the formation of the green SiC and the respective influencing factors during LSI.

Reactions between the solid carbon (C) and the liquid silicon (Si) during the silicon infiltration process (represented by the equation $C_{(s)} + Si_{(l)} \rightarrow SiC_{(s)}$), have been sufficiently investigated, explaining the initial wetting of carbon by liquid silicon [6,7], the subsequent reactions forming the SiC and the infiltration of Si through the carbon pores by the capillary forces [8,9]. Mechanism of growth of the reaction formed SiC has also been studied thoroughly by various researchers leading to propositions using diffusion [10–12] or solution-precipitation models [13]. However, the high temperature reactions involving gaseous species during LSI process have not received sufficient focus. In this case,

* Corresponding author.
E-mail address: manikanda.prakasan@uni-a.de (M.P. Prakasan).

https://doi.org/10.1016/j.oceram.2025.100767
Received 24 December 2024; Received in revised form 12 March 2025; Accepted 12 March 2025
Available online 13 March 2025
2666-5395/© 2025 The Authors. Published by Elsevier Ltd on behalf of European Ceramic Society. This is an open access article under the CC BY-NC license (http://creativecommons.org/licenses/by-nc/4.0/).

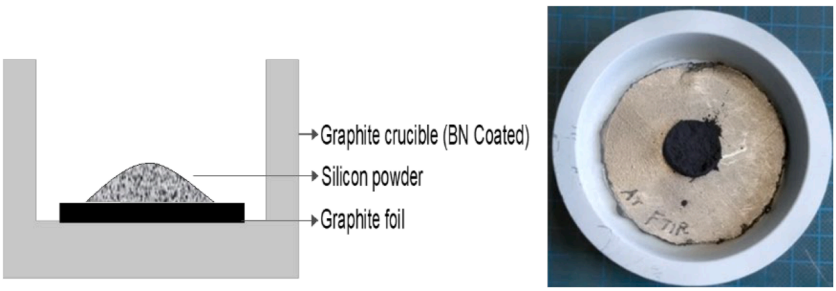

Fig. 1. Experimental set-up in direct contact silicon infiltration (a) schematic (b) picture of the actual set-up.

apart from the starting silicon and the carbon, oxygen is also introduced into the reaction system due to multiple reasons such as moisture and oxides in raw materials, O_2 entrapment in the furnace insulation, contaminations in the inert gas supply and vacuum leaks in the furnace (if present) [5]. There are multiple gas phase reactions possible in a system containing silicon, carbon and oxygen at high temperatures. These reactions are known to strongly depend on the temperature and pressure inside the reaction vessel since they determine the partial pressure of each of the vapor species. Gas phase reactions taking place within a C-Si-O system are not an undiscovered concept. Research by Saito as early as 1992 investigated the formation and growth of SiC whiskers on graphite between 1300 – 1500 °C following the reaction $SiO_{(g)} + 2C_{(s)} \rightarrow SiC_{(s)} + CO_{(g)}$ [14]. Vogli et al. prepared porous silicon carbide (following the same reaction as Saito) by infiltrating a porous carbon substrate with $SiO_{(g)}$ at temperatures between 1550 – 1600 °C under ambient argon atmosphere. There are many other research works dealing with the synthesis of single crystalline SiC fibers following the carbothermal reduction of SiO_2 or by reacting solid silicon with carbon monoxide gas below its melting point. More relevant to silicon melt infiltration process are the following works: Fischedick and Hofbauer proposed the reaction between silicon vapors with solid carbon forming an initial SiC layer on the preform [11,15]; Studies by Israel prove the formation of thin SiC layer on graphite sample held over the silicon melt, due to the transport of Si vapor species at a temperature of 1390 °C under high vacuum (10^{-6} mbar) for 15 min [16]. Favre discussed the gas phase reaction between carbon monoxide (CO) and the liquid silicon to form SiC on the outer surface of the silicon melt [17]; White conducted experiments below the melting point of silicon, by placing a solid silicon piece on a graphite substrate and proved the presence of gas phase reactions from the discolouration and SEM-EDS mapping, showing the silicon carbide depositions on the graphite substrate even upon heating to only 1300 °C [18]; Frolova, on the other hand studied the difference between carbon felts siliconized under vacuum and argon atmosphere, and hypothesized that vacuum encouraged the liquid silicon reaction while argon encouraged the vapor silicon infiltration [19]. Latest research by Hofbauer proved the formation of SiC on the surface of Si particles during LSI at temperatures above 1200 °C under vacuum, using a combination of image processing, SEM-EDS and CO measurement inside the reaction furnace [5]. Despite these research works, there still exists a gap in understanding regarding the influence of gas phase reactions in the outcome of surface siliconization process and a model explaining the possible gaseous reactions before the melting point of silicon is reached. Hence this study aims to confirm the previous observations from literature and extend them with further siliconization experiments, thermo-analytical characterizations and microstructural investigations.

2. Materials and methods

Since this study focuses on investigating the gas phase reactions between silicon and carbon, the methodology is to conduct siliconization experiments of graphite foil substrates in a high temperature furnace to identify the key LSI parameters that influence the process outcome. This is followed by TGA-FTIR analysis of silicon-carbon mixture, for deeper understanding of the reactions taking place before the melting point of silicon. Finally, a thorough SEM investigation of siliconized graphite foils and the silicon-carbon mixture residue from TGA analysis to comprehend and correlate the resulting SiC microstructure with possible reaction mechanisms.

Table 1
Experimental design to prove the presence of gas phase reactions during silicon infiltration: with graphite foil and silicon of various forms exposed to temperatures below and above melting point of Si.

Experiment No.	C substrate	Silicon	Peak temperature in °C
R1	**Graphite foil**	0–75 μm powder	1410
R2	**Graphite foil**	0–75 μm powder	1600
R3	**Graphite foil**	Wafer	1600
R4	**Graphite foil**	Solid globule[a]	1600

[a] *produced in the TOMac furnace by melting Si particles at 1450 °C under vacuum.*

2.1. Materials

Graphite foil substrate used in the siliconization experiments was of 0.5 mm thickness, 6 cm diameter and 1.0 g/cm^3 bulk density (supplied by Sindlhauser). It has to be noted that these graphite foils were pre-heat treated up to 1600 °C under vacuum for 30 min to remove volatiles present on the surface. Silicon used were powder Si of particle sizes 0–75 μm and 0–10 μm (High Quality grade of 99.8 % purity) supplied by Elkem ASA and Si wafer (semi-conductor grade of 99.9999999 % purity). Both carbon and silicon used for all experiments were pre-dried at 110 °C for 36 h prior to siliconization for moisture removal.

2.2. Siliconization experiments

Siliconization experiments were conducted in a high temperature graphite analytical furnace called Thermo Optical Measuring system – atmosphere controlled (TOMac+), similar to the set-up described in [20]. Direct contact siliconization was carried out by placing the graphite foil at the bottom of a boron nitride (BN) coated graphite crucible with an equal mass of silicon on top (as shown in Fig. 1). Experimental design to prove the presence of gas phase reactions and their dependence on the specific surface of silicon is shown in Table 1. During the high temperature treatment inside the furnace, absolute pressure of 3–6 mbar was maintained under an inert argon gas flow of ~2 L/min. Siliconization experiments have undergone equal heating regimes with a maximum hold time of 45 min at the peak temperature.

The second set of siliconization experiments aim at studying the influence of the initial amount of silicon taken. Here, the silicon powder suspended in water was applied on the surface of the graphite foils to ensure homogenous application. The substrate was then dried sufficiently before transferring to the TOMac+ furnace for the siliconization reaction. The silicon-to-carbon ratios were varied between 3 levels to simulate 1) a silicon deficient condition (< 1:1 molar ratio) 2) a

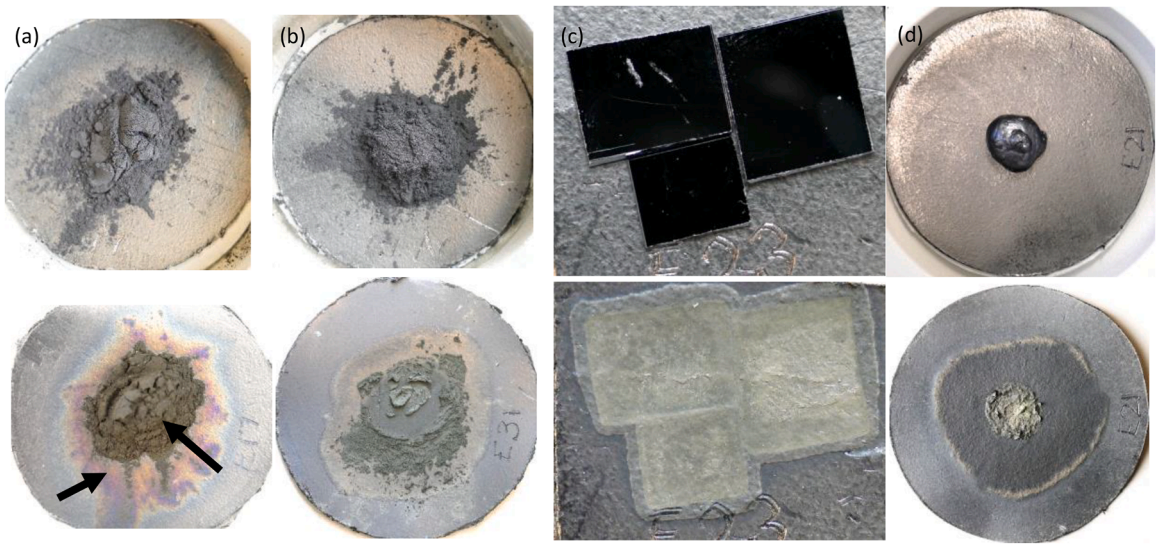

Fig. 2. Before (top) and after (bottom) images of siliconized graphite foils treated (a) at temperature 1410 °C with Si powder – R1 (b) at temperature 1600 °C with Si powder – R2 (c) at temperature 1600 °C with Si wafer – R3 (d) at temperature 1600 °C with solid Si globule – R4.

stoichiometrically sufficient silicon for the complete conversion of the carbon substrate (~1:1 molar ratio) and 3) an excess silicon supply (> 1:1 molar ratio).

2.3. Thermogravimetric analysis with fourier transform infrared spectroscopy

Thermogravimetric Analysis (TGA) was carried out using STA 449 F3 Jupiter from NETZSCH. Two samples (1) with plain fine 0–10 μm Si powder and (2) a mixture containing equal weights of fine 1–5 μm graphite powder and fine 0–10 μm Si powder were heated in a standard Alumina crucible (Al_2O_3, 0.3 ml vol) up to 1405 °C (under 20 ml/min argon purge). Along with the thermogravimetric signal, the gaseous reaction products were also analyzed using an integrated Bruker FT-IR analyzer to capture the CO_2 and CO signals in the exhaust gas stream. FTIR data was analyzed using OPUS software and integrated with the TGA data using Proteus Analysis Software. The heating program used was 25 °C to 800 °C at 30 K/min, 800 to 1405 °C at 10 K/min.

2.4. Microstructural characterization of the siliconized samples

The electron micrographs were recorded in Thermofischer Prisma E scanning electron microscope (SEM) and the high-resolution electron micrographs were recorded by Zeiss Merlin SEM using a Secondary Electron detector. The material composition was analyzed using Energy Dispersive Spectroscopy (EDS) in SEM using a Back Scattered Electron detector.

2.5. SiC particle size calculation using K-means clustering and contour analysis on SEM images

The size of the SiC particles distributed in the Si matrix were calculated from the SEM micrographs using k-means clustering. Contour detection was used to differentiate the silicon carbide particles dispersed within the silicon matrix. The grayscale SEM image underwent histogram equalization and Gaussian blurring to enhance the contrast and reduce the noise. K-means clustering (with three clusters for SiC, Si and embedding resin used) segmented the image by intensity, isolating the SiC regions. Contours of these segments were detected and color-coded, allowing particle boundaries to be identified and measured. Square ROIs were defined, focusing the analysis on target areas. Particle sizes within the ROI were calculated as enclosed contour areas, providing the particle size distributions for each region.

3. Results

3.1. Formation of green SiC during siliconization

All the four siliconization experiments conducted with the graphite foil show the formation of the SiC that is green in colour (refer Fig. 2 for the before and after images of the siliconized samples and Fig. 3 for the corresponding SEM micrographs). Comparing R1 and R2, the impact of

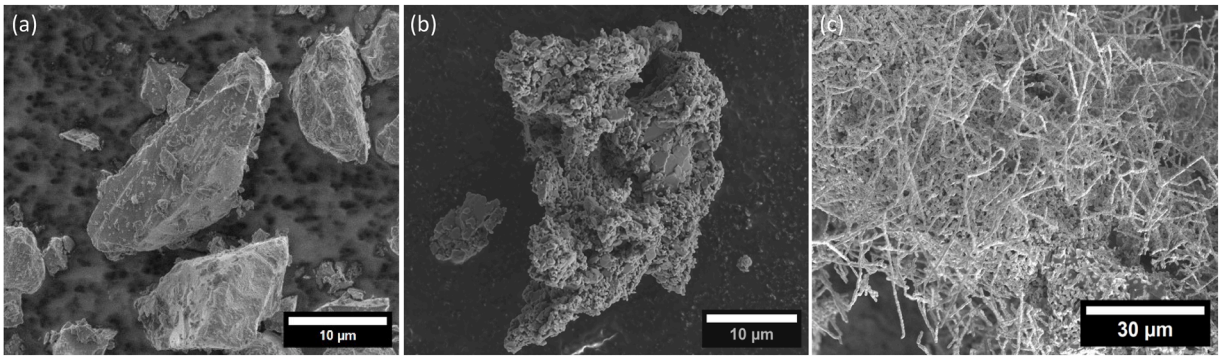

Fig. 3. SEM Micrograph of (a) silicon particle before siliconization (b) silicon particle after siliconization at 1410° (R1) showing porous silicon carbide formation (c) graphite foil after siliconization at 1600 °C with solid silicon globule (R4) showing SiC whiskers.

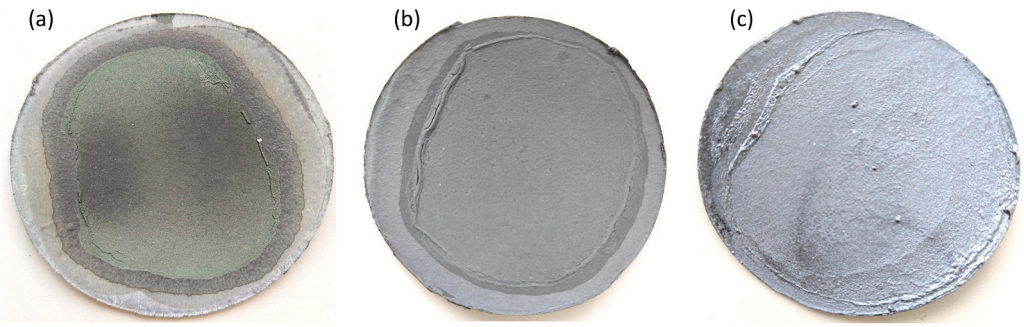

Fig. 4. Images of graphite foil siliconized at 1600 °C with (a) silicon deficient condition showing green surface (b) nearly stoichiometric silicon supply showing grey surface and (c) excess silicon showing silver surface.

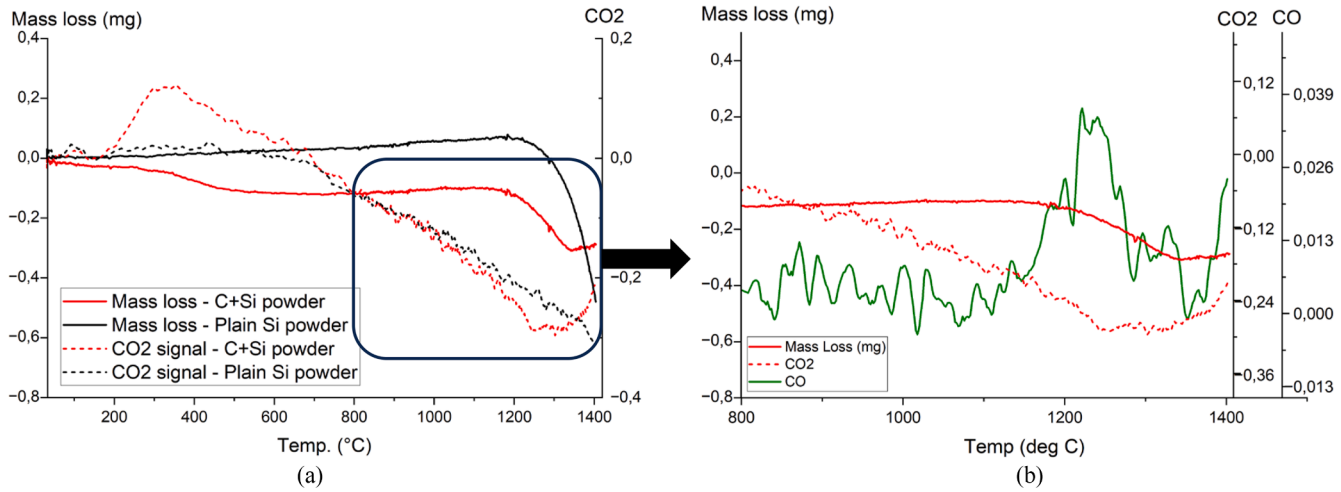

Fig. 5. (a) Overlaid TGA & FTIR curves of plain silicon powder and silicon + carbon powder mixture showing mass loss and CO_2 signals (b) Enlarged TGA & FTIR curves of silicon + carbon powder mixture in the temperature range 800 – 1405 °C, showing mass loss changes and corresponding CO and CO_2 concentrations in exhaust gas.

the reaction temperature is seen indicating the occurrence of green SiC before the melting of silicon. This proves the presence of the gas phase reactions in the reaction system, that lead to the SiC even before the intended reaction of liquid silicon with the carbon substrate. Examination of the green powder deposit on the graphite foil in R1 showed the presence of unreacted, unmelted silicon particles within the heap. SiC formation was seen on the exposed surface of the powder bulk and on the graphite foil surface that was directly in contact with the silicon particles (as discolouration under the green SiC, indicated by arrows in the image). This confirms two distinct gas phase reactions between vapor C species with the Si particles and vapor Si species with the C substrate.

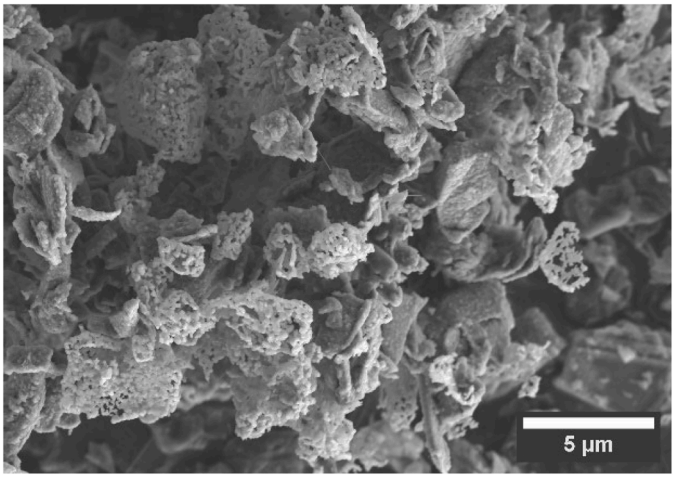

Fig. 6. SEM micrograph of C+Si powder mixture residue from TGA analysis showing porous SiC formation at 1405 °C.

Evaluating the outcome of the experiments R2 - 4, there is a diminution in the extent of green SiC with reducing specific surface of silicon used, with the Si powder resulting in powdery mass of SiC that can easily be scratched out from the substrate surface and the solid Si generating the least green SiC that was still intact on the surface. Corresponding SEM investigations reveal differing SiC morphologies (shown in Fig. 3), in the form of porous shells around the Si particle to whiskers on the siliconized graphite foil.

3.2. *Influence of the amount of initial silicon*

The experiments with differing silicon-to-carbon ratios resulted in a homogenous SiC surface on the graphite foils ranging from green to grey to silver colour (ref Fig. 4). Graphite foil treated under the silicon deficient condition turned green while the excess amount of silicon yielded a silver surface. Nearly stoichiometric silicon supply resulted in a dense grey SiC surface.

3.3. *Thermal analysis of carbon and silicon powder mixture*

TGA curves with overlaid CO_2 signals from the FTIR analysis (refer

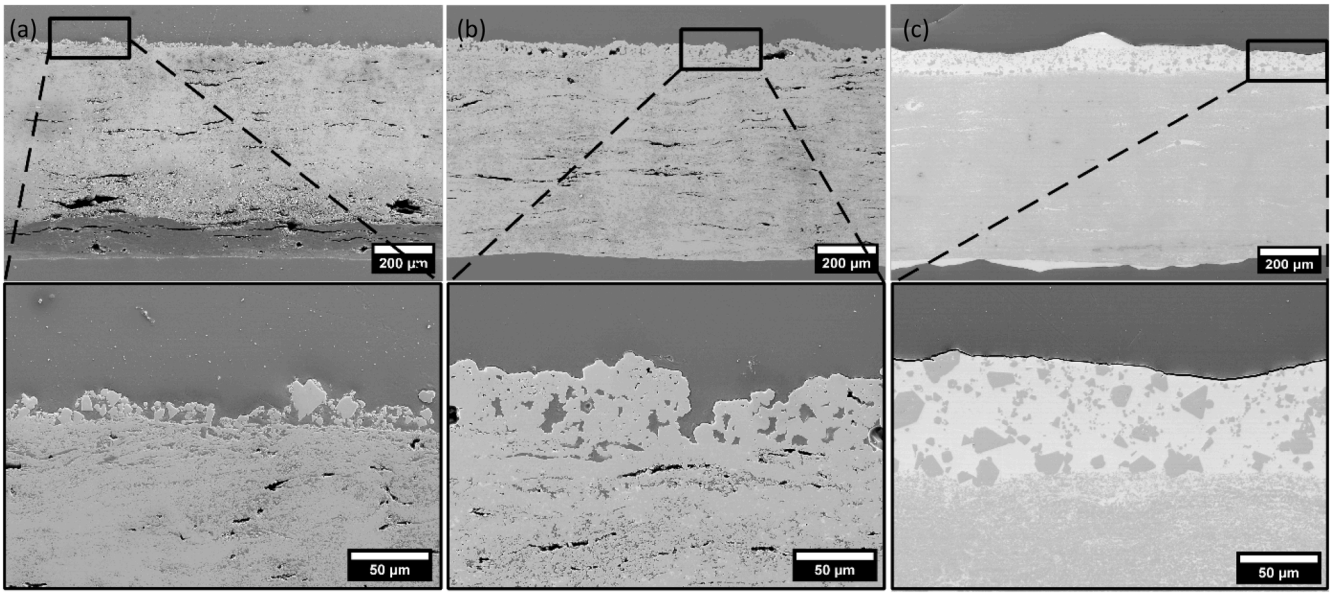

Fig. 7. Polished cross-sectional SEM images of graphite foil siliconized at 1600 °C showing (a) green surface (b) grey surface (c) silver surface at 75x and 400x magnifications.

Fig. 5a) show that plain Si powder shows an initial weight gain between 400 and 880 °C, followed by a swift weight loss between 1200 and 1405 °C. C+Si powder mixture, on the contrary, showed an initial weight loss between 300 and 800 °C, followed by stable behaviour and then again a weight loss trend after 1200 °C. This weight loss after 1200 °C shows a corresponding increase in the CO concentration and a reduction in the CO_2 in the exhaust gas stream (shown in Fig. 5b), which is not seen in the plain Si powder. However, this weight loss is inverted and stabilized at the temperature range of 1330–1405 °C (also shown in Fig. 5b). This region recorded a corresponding increase in the CO_2 and a reduction in the CO signal. The significant difference in the residual weights as well as the thermal response patterns of the two samples (especially in the temperature range of 1300–1400 °C), indicate a different set of reactions forming an additional condensed product in the C+Si mixture. Examination of the residue under SEM-EDS proved this product to be SiC of porous morphology (refer Fig. 6).

3.4. Microstructural investigation of the siliconized surfaces

This section deals with the in-depth SEM investigation of various siliconized specimens, in order to understand the microstructural difference between the green, grey and silver siliconized surfaces and correlate them back to the reaction mechanism responsible for their formation. Samples examined here belong to the silicon infiltration experiment described under Section 3.2 with varying silicon-to-carbon ratios and the graphite foil treated with silicon wafer at 1600 °C (experiment R3 under Section 3.1).

SEM images of the siliconized graphite foils in the cross-sectional view are presented in Fig. 7. The overview images at 75x magnification show the increasing extent of silicon infiltration from green to grey siliconized foil. The green specimen reveals incomplete infiltration while the grey foil is completely infiltrated. Both these however still retain open pores. The silver specimen, on the contrary, is completely infiltrated and has accumulated an excess of silicon on its surfaces as well in the pores, as expected. There are also observable SiC crystals scattered within the excess silicon on the surface (Fig. 7c). Close examination of the surface at 400x reveals the microstructure and adhesion of the siliconized surface with the substrates. The green specimen presents a distinctly detached surface layer constituting a smaller powdery mass of SiC particles with poor adhesion to the substrate. This is also confirmed in the top view SEM examination (in Fig. 8a). Meanwhile, the grey specimen appears to have a porous SiC on the surface (as seen in top-view in Fig. 8b), but in reality, preserves a dense underlayer having good adhesion with the substrate (as seen in the magnified cross-sectional image in Fig. 7b). One of the notable differences between the green and the grey SiC surface is the relative size of the SiC particles, with the green surface consisting of fine SiC particles and the grey coarse SiC particles (comparing Fig. 8a & b).

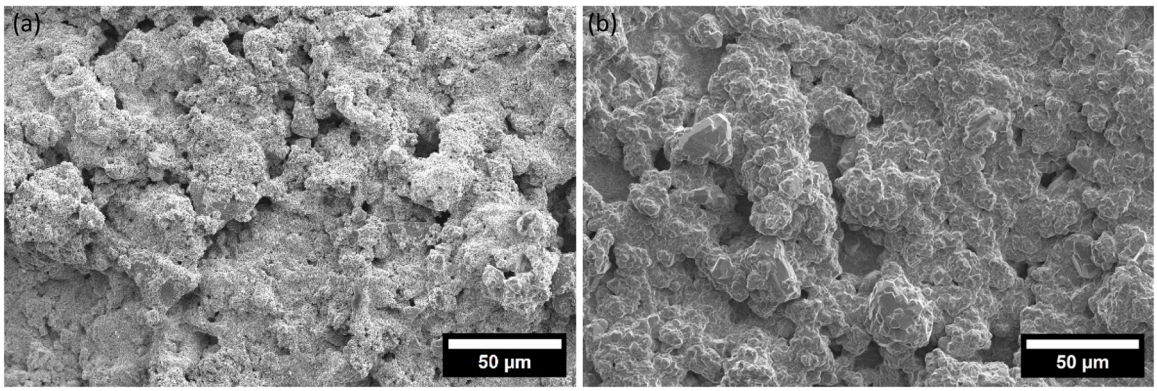

Fig. 8. Top view SEM images of graphite foil siliconized at 1600 °C showing (a) green surface (b) grey surface.

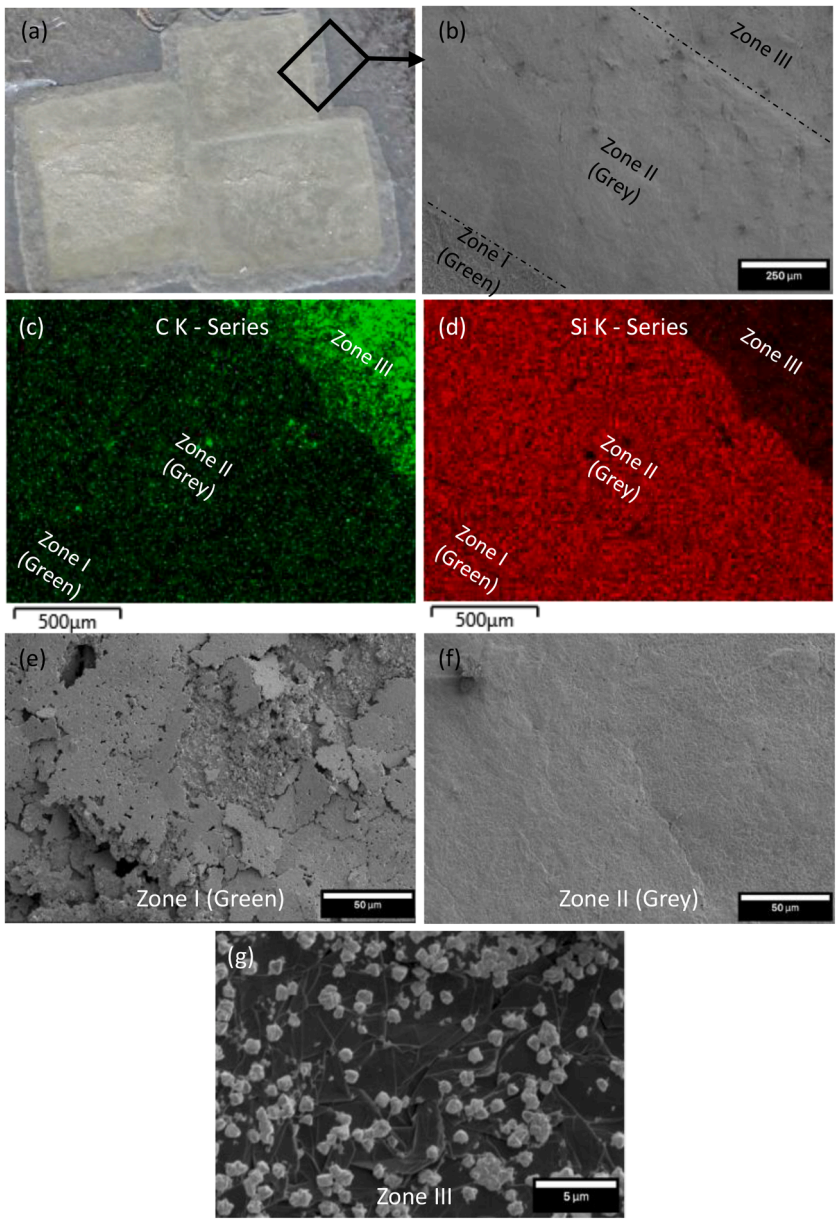

Fig. 9. Graphite foil siliconized with silicon wafer at 1600 °C (Experiment R3)
(a) Image of siliconized graphite foil with the investigated zone highlighted within the black rectangle
(b) SEM overview of Zones I, II & III
(c) SEM-EDS map of C-K series in Zone I, II & III
(d) SEM-EDS map of Si-K series in Zone I, II & III
(e) Magnified SEM image of Zone I showing Green SiC directly under the Si wafer
(f) Magnified SEM image of Zone II showing Grey SiC extending from green SiC
(g) Magnified SEM image of Zone III showing Small SiC particles deposited on the Graphite foil away from the siliconized zones.

Table 2
Composition analysis using SEM-EDS of SiC from different regions of graphite foil siliconized with silicon wafer at 1600° in TOMac+ (experiment R3).

Zone	C weight%	Si weight%
Zone I (Green SiC)	32.5	67.5
Zone II (Grey SiC)	33.5	66.5
Zone III (Graphite foil with SiC agglomerates)	81.8	18.2

Secondly, examination of the graphite foil treated with silicon wafer at 1600 °C (experiment R3) leads to a similar deduction. This specimen shows a distinct green SiC (Zone I) and a grey SiC (Zone II) located adjacent to each other (Fig. 9a-c), with the green surface presenting a porous nature (Fig. 9d) and the grey presenting a dense structure (Fig. 9e). This observation regarding the green SiC in this experiment is identical to the SiC generated by reacting CO with Si wafers at 1100–1400 °C in the study by Antipov et al. [21]. There is also a third region (Zone III) that shows smaller SiC agglomerates on the surface of the graphite foil away from the initial location of the silicon wafer (Fig. 9f), strongly indicating the gaseous propagation of Si during the course of the siliconization process. SEM-EDS investigations of these 3 zones corroborate the findings (refer Table 2).

4. Discussion

4.1. Formation of the green SiC during siliconization and the influencing factors

Experimental results from runs R1 & R2 clearly prove the formation of the green SiC on the surface of the silicon particles below the melting point of silicon. If we consider R2 (treated at 1600 °C) as being one step after R1 (treated at 1410 °C), then it can be ascertained that upon heating to 1600 °C, the green SiC formed on the surface of the silicon particles remains on the surface of graphite foil, after the residual/unreacted silicon melts and infiltrates into the substrate. Comparing runs R2–4, purity of the starting silicon material is found to have no impact on the outcome of the siliconization process, since the purest silicon wafer also produced the green SiC. However, there exists the impact of the specific surface of the silicon. Reducing surface area of the silicon leads to a significant reduction in the green SiC formation. Hofbauer in his work had also identified the specific surface area of the silicon particles to be an influencing factor controlling the amount of oxygen released into the reaction system during siliconization [5]. The current study further corroborates this conclusion. The other influencing factor identified is the ratio of initial silicon-to-carbon ratio in the reaction system. Higher initial amount of the silicon means higher amount of the residual silicon remaining post the gas phase reactions. This residual silicon is then available for liquid phase infiltration into the carbon substrate when the reaction temperature crosses the melting point of silicon. Thus, even with comparable specific surface, if the amount/volume of the initial silicon is higher, it results in a different outcome.

4.2. Thermal analyses indicating the gas phase reactions during siliconization process

The initial weight gain observed in the TGA curve of the plain silicon powder could be attributed to the oxidation from the moisture and other oxygen impurities from the argon gas purge. At lower temperatures, wet and dry oxidation of silicon to silicon dioxide is a well discussed thermodynamically feasible reaction [22,23] with a large negative Gibbs free energy values varying from −805.2 kJ/mol at 300 °C to −682.4 kJ/mol at 1000 °C [24]. The weight loss after 1200 °C is expected to be caused by the release of silicon monoxide (SiO) from the decomposition of silicon dioxide (SiO_2) following Eq. (1). This is a known process to generate SiO gas as demonstrated by Vogli et al., where the SiO gas was produced by heating a mixture of silicon and silica [25].

$$Si_{(s)} + SiO_{2(s)} \rightarrow 2SiO_{(g)} \quad (1)$$

[26,27]

In the C+Si mixture, the initial rapid weight loss at 400 °C could be due to the reaction between C and O_2 impurities resulting in a mass loss as CO_2 (also recorded by a prominent CO_2 signal in FTIR). The second weight loss trend observed from 1172 °C, is attributed to the carbothermic reduction of SiO_2 (on the surface of silicon particles) in the presence of carbon, following the below reaction (Eq. (2)), leading to mass loss as SiO and CO. Corresponding increase in the CO concentration is seen from the FTIR analysis of the exhaust gas.

$$SiO_{2(s)} + C_{(s)} \rightarrow SiO_{(g)} + CO_{(g)} \quad (2)$$

Free energy value (ΔG°) = ~ −200 kJ/mol (at 1200 °C) [5].

With increasing temperature, splitting of CO_2 to CO is aided by the carbon following Eq. (3), resulting in further increase in the CO concentration.

$$CO_{2(g)} + C_{(s)} \rightarrow 2CO_{(g)} \quad (3)$$

ΔG° = −105.4 kJ/mol (at 1300 °C) and −139.19 kJ/mol (at 1500 °C) [14]

With the increasing CO partial pressure in the system, it is also possible for a gas phase reduction of the SiO_2 to take place following Eq. (4).

$$SiO_{2(s)} + CO_{(g)} \rightarrow SiO_{(g)} + CO_{2(g)} \quad (4)$$

There are multiple complex reactions possible in the reduction of silicon dioxide at high temperatures, however the study of Sahajwalla et al. and Krstic et al. showed that the initial stages of the reaction is a solid phase reduction following Eq. (2) and it necessitates physical contact between carbon and silica [28] and influenced by the surface area of silica [29,30]. Together, the reactions (2) and (4) result in the loss of silica layer, thus exposing the underlying silicon to the reaction atmosphere within the furnace saturated with CO.

At temperatures close to 1300 °C, the liberated SiO and CO vapor species start reacting within the system to form a condensed product. Apart from the reactant Si and C, the only other thermodynamically favored condensed product at this temperature range in Si-C-O system is the SiC (SiO_2 is already shown to decompose to SiO and CO at temperatures above 1200 °C). These reactions consuming the intermediates (gaseous SiO & CO) to produce the SiC would explain the TG signal stabilization above 1290 °C and the corresponding reduction in the CO level. Gas phase reactions tend to produce pure SiC crystallites which are typically green in color (despite the impurities present in the starting silicon). Microscopic examination of the SiC from the TGA residue is similar to the green SiC powders from experiments R1 and R2, proving that the gas phase reactions are the cause for formation of porous pure green SiC at temperatures between ~1300–1405 °C.

4.3. Differences in the microstructure of green SiC formed from gas-phase reactions

It has been sufficiently discussed and proven in the previous sections that green silicon carbide is formed from gas phase reactions. SEM investigations into the microstructure of this green SiC however presents differing morphologies, from porous shell-like structures on the silicon particles to whiskers or powdery structures on the siliconized substrates. It can be observed that the porous SiC configuration is mostly seen in silicon saturated regions and the whiskery SiC structures are seen in carbon saturated regions. Manifestation of such distinctly different microstructures from gas phase reactions itself indicate the presence of several gaseous reaction paths within the Si-C-O system. This calls for additional deeper deliberations to ascertain the various reaction pathways that generate silicon carbide during the siliconization process.

4.4. Gas phase reactions favoring the formation of SiC before the melting point of silicon

Based on the inferences from experimentation, thermal analyses and microstructural investigations, it is apparent that the reaction system during siliconization is extremely complex, involving the presence of multiple gaseous entities and reaction paths. This study tries to comprehend the same by investigating the thermodynamics of possible high temperature reactions in the Si-C-O system and mapping them to published research works describing the formation of SiC from gas phase reactions. It is already concluded from the previous sections that C, Si and SiC are the three key condensed phases and SiO and CO are the two key vapor species that need to be considered in the temperature range between 1300-$T_{m,Si}$. Since the nature of SiC formed differs based on the substrate and the reaction mechanism, we have attempted to classify them into 3 possible reaction paths accordingly:

Where the CO saturation is high and a reducing substrate is available: The first key reaction is in gas-gas phase, between carbon monoxide and silicon monoxide on or very close to the surface of the carbon substrate. The conditions here are ideal for further carbothermic reactions of the products. Accordingly, the first reaction 5a yields SiC that condenses on

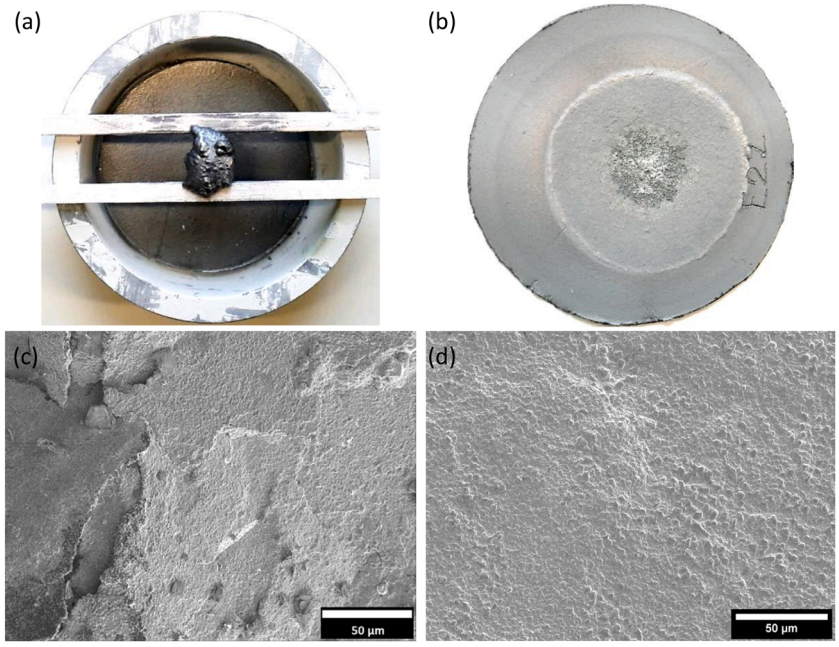

Fig. 10. a) Experimental set-up to minimise gas phase reaction during siliconization (b) resulting siliconized graphite foil without green SiC (c) SEM image of the middle area showing spalled dense SiC layer (d) SEM image of surrounding dense grey SiC without cracks or surface spalling.

the carbon surface while the other product CO_2 is reduced further to CO. It is the highly exergonic 5b reaction that continuously consumes CO_2 making SiC formation more favorable. The combined reaction 5 siliconizes the carbon bulk [28] and can also form SiC whiskers on the surface of carbon substrate [14,31]. It is also one of the established methods for synthesizing pure SiC powders or whiskers on graphite substrates [32] and to siliconize carbonaceous substrates [25].

$$SiO_{(g)} + 3CO_{(g)} \rightarrow SiC_{(s)} + 2CO_{2(g)} \quad (5a)$$

$$CO_{2(g)} + C_{(s)} \rightarrow 2CO_{(g)} \quad (5b)$$

Combining (5a) & (5b), the whole reaction can be written as:

$$SiO_{(g)} + 2C_{(s)} \rightarrow SiC_{(s)} + CO_{(g)} \quad (5)$$

$\Delta G^{\circ} = -78.30$ kJ/mol (at 1300 °C) [14,33,34]

This reaction not only siliconizes the carbon substrate, but is also expected to be responsible for the slow conversion of the graphite heaters and other carbonaceous elements within the siliconization furnace to silicon carbide.

Where the CO saturation is high and a reducing substrate is NOT available: The other thermodynamically favored reaction is between gaseous CO and SiO to form SiC and SiO_2 following reaction (6). This reaction is proven to take place where there is no active carbon or graphite available [14] or when all the carbon in the system is consumed to form SiC during the later part of the reaction 5 [35]. The SiC formed here condenses as green deposits on the reaction crucibles or inner walls of the furnace. SiO_2 condenses on cooler parts of the furnace (such as windows) as powdery deposits ranging from yellow to brown colour.

$$3SiO_{(g)} + CO_{(g)} \rightarrow SiC_{(s)} + 2SiO_{2(s)} \quad (6)$$

$\Delta G^{\circ} = -370.46$ kJ/mol (at 1300 °C) [14,35]

Where the Si saturation is high: On or near the surface of silicon, three possible reactions can take place, resulting in formation of SiC. This SiC builds up as a layer around the silicon and forms a porous shell. The reaction products formed (SiO and O_2) further aid in continuing the gaseous reactions until all available C and Si surfaces are converted to SiC. There are two important consequences to this reaction (i) there is silicon depletion / consumption that makes it unavailable for melting and infiltrating into the carbon substrate (ii) depending upon the thickness of the SiC shell layer, it could trap the unreacted residual silicon within, thus further reducing the silicon availability.

$$2Si_{(s)} + CO_{(g)} \rightarrow SiC_{(s)} + SiO_{(g)} \quad (7a)$$

$$2Si_{(s)} + 2CO_{(g)} \rightarrow 2SiC_{(s)} + O2_{(g)} \quad (7b)$$

$$3Si(s) + 2CO_{(g)} \rightarrow 2SiC_{(s)} + SiO_{2(s)} \quad (7c)$$

In a reaction system with significantly higher amounts of Si than CO ($n \geq 1.5$ mol), reaction 7c is the most feasible at the temperature range from 300 - 2000K. Antipov et al. found this reaction 7c to be the most spontaneous at the temperature close to the melting point of Si (generating green powdery sinter) and a strong direct relationship with the silicon surface area [21]. While the SiC outer layer formed in this reaction traps the silicon inside, the SiO_2 is spontaneously decomposed into SiO and CO in the presence of C, following the Eq. (2) discussed earlier in this study. Hence, apart from supplying the reactive intermediates for the gas phase reactions, the high specific surface of silicon also means higher surface area for reacting with the CO producing SiC (resulting in more silicon depletion that would otherwise be utilized during the liquid silicon infiltration).

4.5. Siliconization experiment with minimized gas phase reactions

From the previous experiments and analyses, it is apparent that the gas phase reactions play a major role in the formation of green SiC layer. Hence to verify this, an experimental set-up was designed to minimize the gas phase reactions during siliconization. This was made possible by an arrangement shown in Fig. 10a, consisting of a graphite foil placed at the bottom of BN coated graphite crucible and a solid Si globule placed directly above the graphite foil with the help of BN coated graphite sticks. This entire set-up was placed in the TOMac+ furnace for siliconization. All the other process parameters were maintained identical to the previous experimentations R2-R4, with the peak temperature at 1600 °C. In this experiment, the graphite and silicon were physically separated until the melting point of silicon was reached, when the solid globule melted and dropped onto the graphite. This was followed by an immediate reaction between the liquid silicon and the solid carbon,

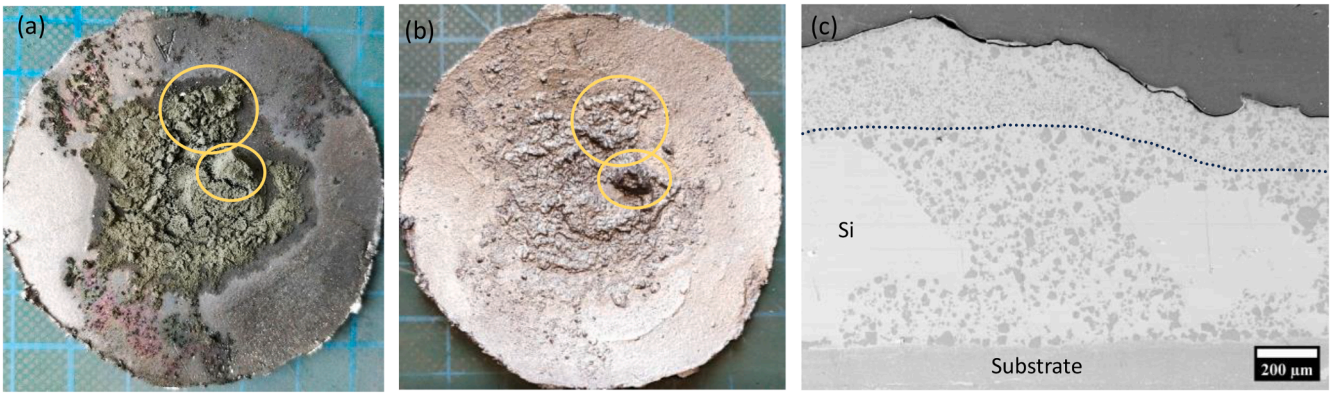

Fig. 11. (a) Graphite foil showing green surface used as starting material (b) reprocessed with excess silicon supply showing silver surface (c) SEM micrograph of polished cross-section of reprocessed foil with silver surface.

minimizing the gas phase reactions. The resultant siliconized graphite foil showed no green porous SiC layer, but only a dense grey SiC (shown in Fig. 10b).

Microstructural investigations revealed a cracked or spalled but dense SiC microstructure in the middle portion of the foil, corresponding to the region where the molten silicon contacted the graphite foil. The abrupt contact of the molten silicon with the graphite causes rapid volume expansion due to SiC formation. This triggers new crack formation and provides fresh pathway for silicon penetration, ultimately causing cleavage of the layered structure of the graphite foil [17]. End result of this brings a non-uniform locally broken SiC layer seen in Fig. 10c. The area surrounding the spalled region is seen to have a dense SiC which is typical for liquid silicon infiltration process.

Absence of the green SiC (of both porous as well as whisker morphology) in this experiment reinforces the hypothesis, that reaction (2) initiated by the reduction of the SiO_2 layer (on the silicon particles) by the carbon, forming the reactive SiO and CO vapor species is essential for triggering the gas phase reactions. By avoiding physical contact between the carbon and the silicon, formation of the SiO and CO was minimized, thus preventing the reaction proceeding in the direction of SiC formation from gas phase reactions. Even if the amount of silicon taken was insufficient to completely infiltrate the carbon substrate, when the gas phase reactions were minimized, it prevented the generation of porous green SiC. It is still possible, that there could be some CO generation from the graphite heating elements of the furnace (due to oxygen impurities reacting with the carbon) and SiO generation from silica reduction following reaction (1), however with proper sample preparation and preventive measures, this could be kept to a minimum, preventing the green SiC formation, as demonstrated in this experiment.

4.6. Siliconization reaction to convert the green surface to silver surface

It is evident from Section 4.5 that the gas phase reactions can be minimised, but cannot be eliminated, unless the starting carbon and silicon are physically separated. Hence there is always some gas phase formation of fine SiC on the silicon particle. However, in the grey and silver coloured siliconized graphite foils (from Section 3.2), there is no trace of the fine crystallites. This implies that the SiC generated from gas phase reactions either disappear or transform their morphology during the melt phase reaction of silicon past its melting point. Therefore, this section describes a siliconization experiment and the subsequent cross-sectional microscopic examination to convert a siliconized graphite foil with green surface into silver by supplying excess silicon.

For the experiment, a siliconized graphite foil with green SiC (previously processed under conditions identical to R2) is used (shown in Fig. 11a). Further excess silicon powder is added on its surface and treated in TOMac+ at 1600 °C. The resulting specimen shows a silver surface with the contour identical to the green one (especially the regions highlighted in the images). Examination of the polished cross-section shows silicon rich areas where silicon carbide is completely absent. These uniquely shaped areas are larger than the 75 µm particle size of starting silicon powder used. They could be attributed to the areas corresponding to the porous SiC shells of the original green surface (surrounding one or more silicon grains), which were later filled with molten silicon during the re-processing step. The infiltration of molten silicon must have preserved their morphology during subsequent sample preparation steps (including cutting and polishing) and SEM investigation, which could have otherwise been destroyed. Another interesting observation in the micrographs is the presence of SiC crystals in the Si matrix. This is similar to the studies of Favre et al. where isolated SiC crystallites were observed in Si matrix on the surface of siliconized carbon substrates. However, there was no conclusion offered regarding their presence or formation [17]. In the current experiment, there exists a difference in the size of SiC particles distributed in the silicon matrix. There are distinctly two groupings, separated by the dotted line in Fig. 11c (1) coarse SiC particles, with an average size of 1.25 μm^2, between the substrate and the dotted line (at the same level as the SiC shells) and (2) finer SiC particles with an average size of 0.29 μm^2, close to the upper surface of the Si (above the level of the SiC shells). The coarse SiC particles could be attributed to the dissolution-precipitation phenomena of the fine green SiC particles (which were originally present on the foil surface along with the SiC shells) in the silicon melt during the reprocessing step [36]. The finer SiC crystallites close to Si surface must be the ones formed due to the gas phase reactions during the reprocessing step and their subsequent dispersion in Si melt.

4.7. Proposed reaction model explaining the gas phase reactions forming the green SiC during the surface silicon infiltration process

The following 4-step mechanism is proposed to describe the sequence of events during the surface silicon infiltration process and to explain the formation of green silicon carbide.

At temperatures below 1200 °C: possible oxidation of the silicon particle surface building up SiO_2 layers; no other significant reaction of consequence other than the loss of moisture and other volatiles from the starting materials.

Between 1200–1300 °C: reduction of the SiO_2 in the presence of carbon, releasing gaseous SiO and CO. Loss of the oxide layer exposes the silicon surface to the furnace atmosphere. The specific surface of silicon impacts this step by influencing the amount of SiO & CO released and by making the surface of the silicon particles available for reaction with CO.

Between 1300 °C – T_m of Si: Gas phase reactions (Equations (5) – (7)) forming the green porous SiC on the surface of silicon particles (as shells), on the carbon substrate (as whiskers or agglomerates) and within the inner walls of the reaction vessel/furnace as green SiC condensates.

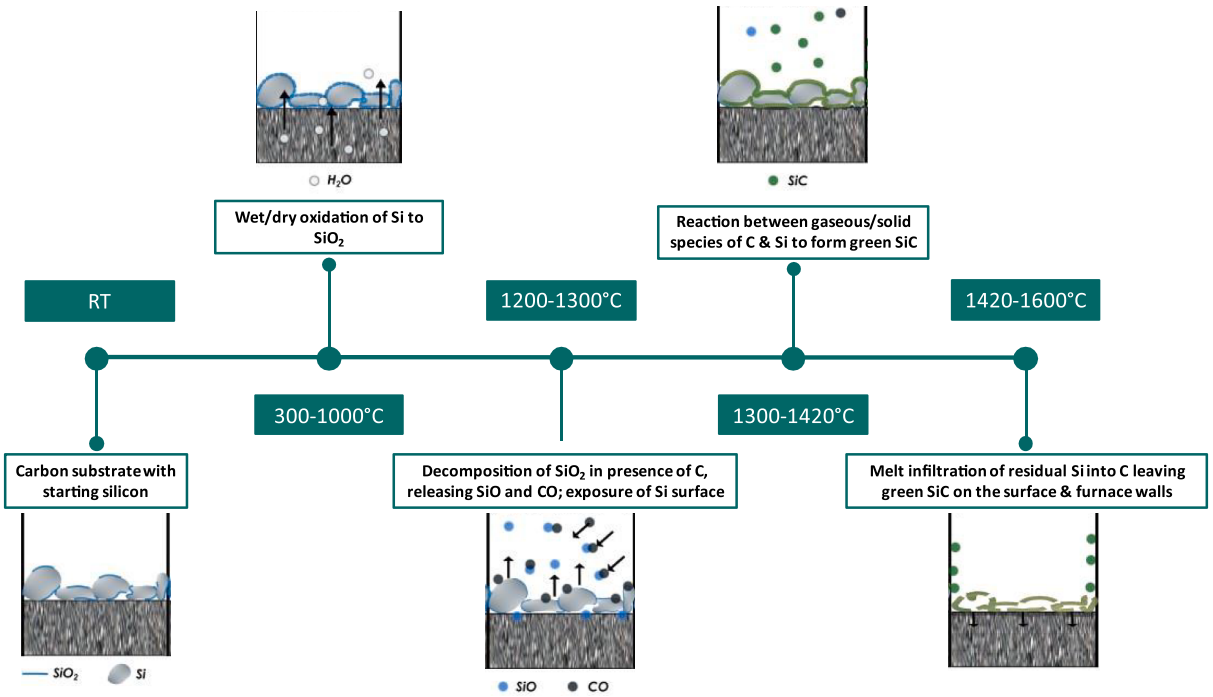

Fig. 12. Schematic illustration of proposed reaction model explaining gas phase reactions forming green SiC.

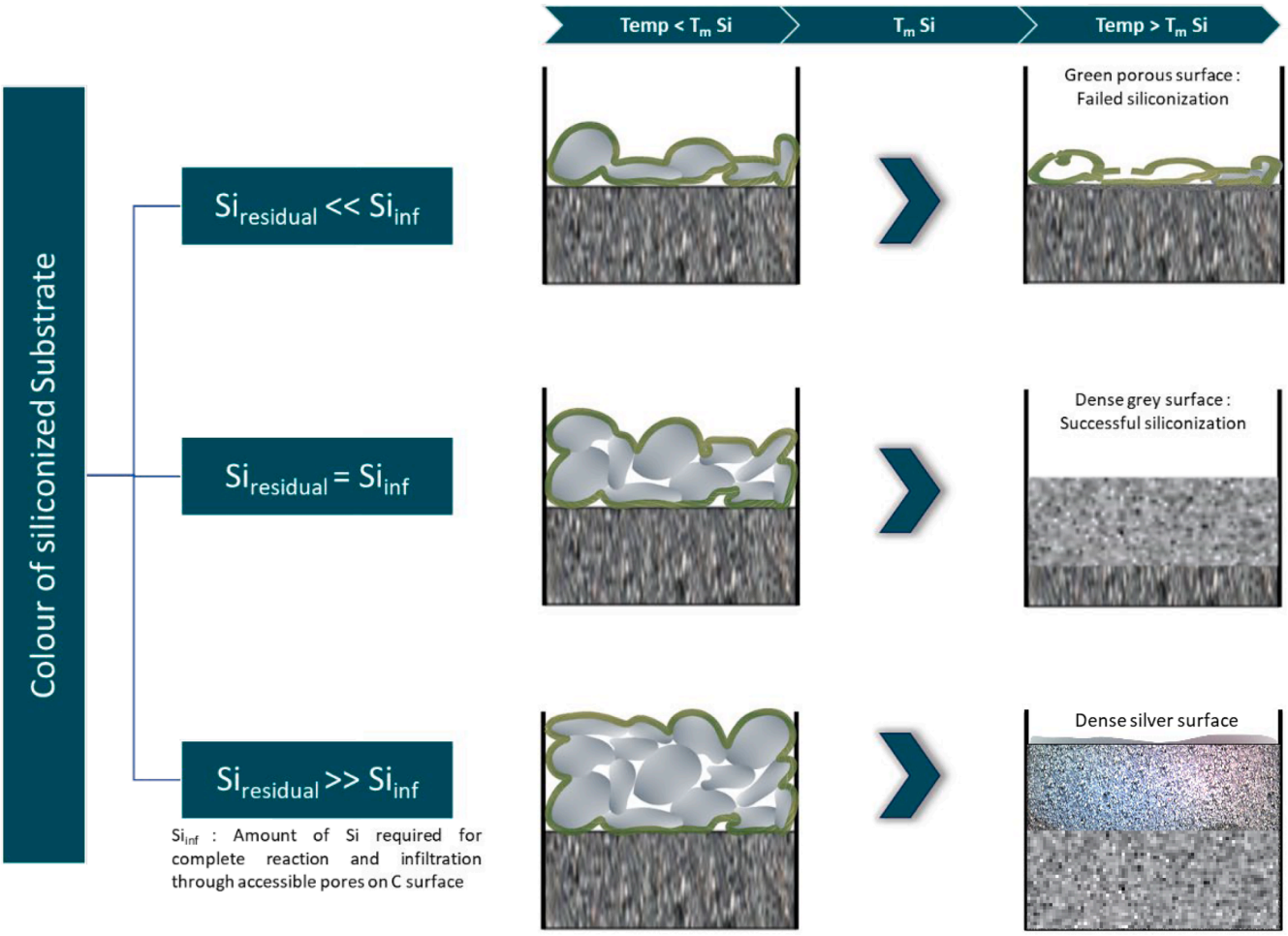

Fig. 13. Schematic illustration explaining the formation of green, grey and silver coloured surfaces after siliconization process.

Between T_m of Si – 1600 °C: melting of the residual unreacted silicon and liquid infiltration into the carbon substrate forming a dense SiC surface. The green porous SiC shells that were formed around the silicon particles remain on the siliconized surface as green powdery deposits. Depending on the amount of the residual silicon there are three possible outcomes (i) when there is no or only negligible amount of the residual silicon: the green SiC stays intact as powdery mass on the surface of the carbon substrate → ***failed surface siliconization***. Sometimes, even where there is substantial amount of residual silicon available, it is possible that it is completely entrapped within a thick SiC shell (making it unavailable for infiltration) (ii) when the amount of residual silicon is sufficient to infiltrate and react with the carbon substrate, there is a dense SiC layer formed due to liquid phase reaction → ***successful surface siliconization***. There is a likelihood of the finer green SiC crystals formed from gas phase reactions to dissolve in the silicon melt and re-precipitate as coarser crystals on the surface. Addition of impurities from the Si melt during this dissolution-precipitation converts the green SiC to grey SiC. Thus, the entire surface appears grey (iii) When the amount of residual Si is much higher than the amount required to completely convert the surface of carbon substrate, there is accumulation of molten silicon on the surface. Such substrates with excess silicon appear silver. Though this surface layer possesses good adhesion with the substrate and is devoid of the porous SiC, presence of elemental silicon could adversely impact the high temperature resistance of the siliconized component. On an added note, the microstructure of carbon substrate (in terms of porosity, pore size and extent of the cracks open to the surface) could have a significant influence on this step, by determining the amount of silicon consumed during infiltration. Highly porous substrates require higher amount of silicon than a corresponding substrate with low porosity, for producing a SiC surface of identical thickness.

The above proposed reaction progression is represented schematically in Fig. 12. The exact temperature of each step could vary depending on the furnace pressure (whether carried out under low vacuum or atmospheric pressure under argon purging) and the partial pressures of O_2 and CO. However, the sequence would remain the same. The outcome of the entire process in terms of the color of siliconized surface based on the amount of residual silicon available for infiltration is illustrated in Fig. 13, with the porous green SiC termed as a failed sample, that needs to be reworked to obtain a dense SiC surface.

5. Conclusions

This study explores the challenges of the reactive melt infiltration of carbon substrates with silicon, particularly the formation of silicon carbide mediated by gas-phase species, which adversely affects the surface siliconization process. Through experiments and thermal analyses, it is verified that the carbothermic reduction of silicon dioxide present on the silicon particles and the gas phase reactions between silicon and carbon monoxide within the reaction system, play a key role in the formation of the green coloured SiC layer on the siliconized substrates. Factors such as the specific surface of silicon and the amount of residual silicon post the gas phase SiC formation influence these reactions. Minimizing the gas phase reactions can prevent greenish surface layers of the processed substrates/composites. The proposed reaction mechanism sheds light on the intricate process, offering insights into the occurrence of green, grey, and silver coloured siliconized components during the surface silicon infiltration process.

CRediT authorship contribution statement

Manikanda Priya Prakasan: Writing – original draft, Project administration, Methodology, Investigation, Formal analysis, Data curation. **Tobias Schneider:** Writing – review & editing, Methodology, Conceptualization. **Dietmar Koch:** Writing – review & editing, Validation, Supervision, Resources.

Declaration of competing interest

The authors declare that they have no known competing financial interests or personal relationships that could have appeared to influence the work reported in this paper.

Acknowledgements

The authors acknowledge the financial support from the Deutsche Forschungsgemeinschaft (DFG funding/Project number 454647179) for funding the high temperature graphite analytical furnace used in this study.

References

[1] W. Krenkel, Carbon fibre reinforced silicon carbide composites (C/SiC, C/C-SiC). Handbook of Ceramic Composites, Springer, Boston, MA, 2005, pp. 117–148, https://doi.org/10.1007/0-387-23986-3_6.
[2] G. Savage, Oxidation and oxidation protection. Carbon-Carbon Composites, Springer, Dordrecht, 1993, pp. 193–225, https://doi.org/10.1007/978-94-011-1586-5_6.
[3] G.W. Meetham, High-temperature materials — a general review, J. Mater. Sci. 26 (1991) 853–860, https://doi.org/10.1007/BF00576759.
[4] T. Aoki, H. Hatta, Y. Kogo, H. Fukuda, Y. Goto, T. Yarii, High temperature oxidation behavior of SiC-coated C/C composites, J. Japan Inst. Metals 62 (1998) 404–412, https://doi.org/10.2320/JINSTMET1952.62.4_404.
[5] Hofbauer P.J., Raether F. Effects of oxygen on the Liquid Silicon Infiltration (LSI) process. Open Ceram.. 2023;14:100337. doi:10.1016/j.oceram.2023.100337.
[6] A. Casado, J. Torralba, S. Milenkovic, Wettability and infiltration of liquid silicon on graphite substrates, Metals. 9 (2019) 300, https://doi.org/10.3390/met9030300.
[7] A. Ciftja, T.A. Engh, M. Tangstad, Wetting properties of molten silicon with graphite materials, Metall. Mat. Trans. A 41 (2010) 3183–3195, https://doi.org/10.1007/s11661-010-0362-8.
[8] F.H. Gern, R. Kochendörfer, Liquid silicon infiltration: description of infiltration dynamics and silicon carbide formation, Appl. Sci. Manufact. 28 (1997) 355–364, https://doi.org/10.1016/S1359-835X(96)00135-2.
[9] S. Kumar, A. Kumar, R. Devi, A. Shukla, A.K. Gupta, Capillary infiltration studies of liquids into 3D-stitched C–C preforms, J. Eur. Ceram. Soc. 29 (2009) 2651–2657, https://doi.org/10.1016/j.jeurceramsoc.2009.03.006.
[10] H. Zhou, R.N. Singh, Kinetics model for the growth of silicon carbide by the reaction of liquid silicon with carbon, J Am. Cer. Soc. 78 (1995) 2456–2462, https://doi.org/10.1111/j.1151-2916.1995.tb08685.x.
[11] J. Schulte-Fischedick, A. Zern, J. Mayer, M. Rühle, M. Frieß, W. Krenkel, R. Kochendörfer, The morphology of silicon carbide in C/C–SiC composites, Mater. Sci. Eng. 332 (2002) 146–152, https://doi.org/10.1016/S0921-5093(01)01719-1.
[12] Li Zhuan, Zhu Zi-bing, Xiao Peng, Xiong Xiang. The morphology and mechanism of formation of SiC in C/C-SiC composites fabricated by liquid silicon infiltration, J. Cer. Process. Res. 11 (2010) 335–340, https://doi.org/10.36410/JCPR.2010.11.3.335.
[13] R. Pampuch, E. Walasek, J. Bialoskórski, Reaction mechanism in carbon-liquid silicon systems at elevated temperatures, Ceram. Int. 12 (1986) 99–106, https://doi.org/10.1016/0272-8842(86)90023-4.
[14] M. Saito, S. Nagashima, A. Kato, Crystal growth of SiC whisker from the SiO(g)-CO system, J. Mater. Sci. Lett. 11 (1992) 373–376, https://doi.org/10.1007/BF00728713.
[15] P.J. Hofbauer, E. Rädlein, F. Raether, Fundamental mechanisms with reactive infiltration of silicon melt into carbon capillaries, Adv. Eng. Mater. 21 (2019) 1900184, https://doi.org/10.1002/adem.201900184.
[16] R. Israel, R. Voytovych, P. Protsenko, B. Drevet, D. Camel, N. Eustathopoulos, Capillary interactions between molten silicon and porous graphite, J. Mater. Sci. 45 (2010) 2210–2217, https://doi.org/10.1007/s10853-009-3889-6.
[17] A. Favre, H. Fuzellier, J. Suptil, An original way to investigate the siliconizing of carbon materials, Ceram. Int. 29 (2003) 235–243, https://doi.org/10.1016/S0272-8842(02)00110-4.
[18] J.F. White, L. Ma, K. Forwald, Du Sichen, Reactions between silicon and graphite substrates at high temperature: in situ observations, Metall. Materi. Trans. B 45 (2014) 150–160, https://doi.org/10.1007/s11663-013-9947-0.
[19] M.G. Frolova, A.S. Lysenkov, D.D. Titov, K.A. Kim, A.Y. Ivannikov, S.N. Perevislov, Y.F. Kargin, Influence of the gas atmosphere on the formation of SiC fibers upon the siliconization of carbon felt, Russ. J. Inorg. Chem. 66 (2021) 1191–1195, https://doi.org/10.1134/S0036023621080052.
[20] F. Raether, R. Hofmann, G. Müller, H.J. Sölter, A novel thermo-optical measuring system for the in situ study of sintering processes, J. Therm. Anal. Calorim. 53 (1998) 717–735, https://doi.org/10.1023/A:1010111023658.
[21] A.V. Antipov, R.G. Pavelko, V.G. Sevast'yanov, N.T Kuznetsov, Thermodynamic and experimental study of the interaction of silicon and carbon monoxide: synthesis of silicon carbide nanofibers, Russ. J. Inorg. Chem. 56 (2011) 1517–1524, https://doi.org/10.1134/S0036023611100032.
[22] H.Z. Massoud, The onset of the thermal oxidation of silicon from room temperature to 1000°C, Microelectron. Eng. 28 (1995) 109–116, https://doi.org/10.1016/0167-9317(95)00026-5.

[23] V.K. Bhat, M. Pattabiraman, K.N. Bhat, A. Subrahmanyam, The growth of ultrathin oxides of silicon by low temperature wet oxidation technique, Mater. Res. Bull. 34 (1999) 1797–1803, https://doi.org/10.1016/S0025-5408(99)00158-0.
[24] M. Nagamori, I. Malinsky, A. Claveau, Thermodynamics of the Si-C-O system for the production of silicon carbide and metallic silicon, Metall Trans. B 17 (1986) 503–514, https://doi.org/10.1007/BF02670216.
[25] E. Vogli, J. Mukerji, C. Hoffman, R. Kladny, H. Sieber, P. Greil, Conversion of oak to cellular silicon carbide ceramic by gas-phase reaction with silicon monoxide, J. Am. Cer. Soc. 84 (2001) 1236–1240, https://doi.org/10.1111/j.1151-2916.2001.tb00822.x.
[26] O. Kubaschewski, T.G. Chart, Silicon monoxide pressures due to the reaction between solid silicon and silica, J. Chem. Thermodyn. 6 (1974) 467–476, https://doi.org/10.1016/0021-9614(74)90008-1.
[27] K.M. O'Connor, A. Rubletz, J. Trach, C. Butler, J.G.C. Veinot, Understanding silicon monoxide gas evolution from mixed silicon and silica powders, Nanoscale Horiz. (2023) 892–899, https://doi.org/10.1039/d3nh00076a.
[28] V. Sahajwalla, C. Wu, R. Khanna, N.S. Chaudhury, J. Spink, Kinetic study of factors affecting in situ reduction of silica in carbon-silica mixtures for refractories, ISIJ Int 43 (2003) 1309–1314, https://doi.org/10.2355/isijinternational.43.1309.
[29] V.D. Krstic, Production of fine, high-purity beta silicon carbide powders, J Am. Cer. Soc. 75 (1992) 170–174, https://doi.org/10.1111/j.1151-2916.1992.tb05460.x.
[30] Agarwal A., Pad U. Influence of pellet composition and structure on carbothermic reduction of silica. Metall and Materi Trans B. 1999;30:295–306. doi:10.1007/s11663-999-0059-9.
[31] C. Vix-Guterl, P. Ehrburger, Effect of the properties of a carbon substrate on its reaction with silica for silicon carbide formation, Carbon. N. Y. 35 (1997) 1587–1592, https://doi.org/10.1016/S0008-6223(97)00117-6.
[32] B.M. Moshtaghioun, A. Monshi, M.H. Abbasi, F. Karimzadeh, The effect of crystallinity of carbon source on mechanically activated carbothermic synthesis of nano-sized SiC powders, J. of Materi Eng and Perform. 22 (2013) 421–426, https://doi.org/10.1007/s11665-012-0296-y.
[33] N. Klinger, Strauss EL, Komarek KL, Reactions between silica and graphite, J Am. Ceram. Soc. 49 (1966) 369–375, https://doi.org/10.1111/j.1151-2916.1966.tb13287.x.
[34] X. Li, G. Zhang, O. Ostrovski, R. Tronstad, Effect of gas atmosphere on the formation of silicon by reaction of SiC and SiO2, J. Mater. Sci. 51 (2016) 876–884, https://doi.org/10.1007/s10853-015-9413-2.
[35] N.S. Jacobson, E.J. Opila, Thermodynamics of Si-C-O system, Metall Trans A 24 (1993) 1212–1214, https://doi.org/10.1007/BF02657254.
[36] J. Roger, A. Marchais, Y. Le Petitcorps, Examination of the interaction between liquid silicon and bulk silicon carbide, J. Cryst. Growth 426 (2015) 1–8, https://doi.org/10.1016/j.jcrysgro.2015.05.013.